

# Spin reorientation and disordered rare earth magnetism in $\text{Ho}_2\text{FeCoO}_6$

**Haripriya G. R.<sup>1</sup>, Harikrishnan S. Nair<sup>2</sup>, Pradheesh R.<sup>1\*</sup>, S. Rayaprol<sup>3</sup>, V. Siruguri<sup>3</sup>, Durgesh Singh<sup>4</sup>, R. Venkatesh<sup>4</sup>, V. Ganesan<sup>4</sup>, K. Sethupathi<sup>1</sup>, V. Sankaranarayanan<sup>1</sup>**

<sup>1</sup>Low Temperature Physics Laboratory, Department of Physics, Indian Institute of Technology Madras, Chennai-600036, India

<sup>2</sup> Department of Physics, 500 West University Ave, University of Texas at El Paso, TX 79968, USA

<sup>3</sup> UGC-DAE Consortium for Scientific Research - Mumbai Centre, R-5 Shed, BARC Campus, Mumbai-400085, India

<sup>4</sup>Low Temperature Laboratory, UGC-DAE Consortium for Scientific Research, University Campus, Khandwa Road, Indore-452001, India

\*Current address: Department of Physics, National Institute of Technology Calicut, Kozhikode - 673601, Kerala, India

E-mail: ksethu@iitm.ac.in, haripriya@physics.iitm.ac.in

**Abstract.** We report the experimental observation of spin reorientation in the double perovskite  $\text{Ho}_2\text{FeCoO}_6$ . The magnetic phase transitions in this compound are characterized and studied through magnetization and specific heat, and the magnetic structures are elucidated through neutron powder diffraction. Two magnetic phase transitions are observed in this compound – one at  $T_{\text{N1}} \approx 250$  K, from paramagnetic to antiferromagnetic, and the other at  $T_{\text{N2}} \approx 45$  K, from a phase with mixed magnetic structures to a single phase through a spin reorientation process. The magnetic structure in the temperature range 200 K – 45 K is a mixed phase of the irreducible representations  $\Gamma_1$  and  $\Gamma_3$ , both of which are antiferromagnetic. The phase with mixed magnetic structures that exists in  $\text{Ho}_2\text{FeCoO}_6$  gives rise to a large thermal hysteresis in magnetization that extends from 200 K down to the spin reorientation temperature. At  $T_{\text{N2}}$ , the magnetic structure transforms to  $\Gamma_1$ . Though long-range magnetic order is established in the transition metal lattice, it is seen that only short-range magnetic order prevails in  $\text{Ho}^{3+}$ – lattice. Our results should motivate further detailed studies on single crystals in order to explore spin reorientation process, spin switching and the possibility of anisotropic magnetic interactions giving rise to electric polarization in  $\text{Ho}_2\text{FeCoO}_6$ .

*Keywords:* spin reorientation, disordered double perovskite, mixed magnetic structures

Submitted to: *J. Phys.: Condens. Matter*

## 1. Introduction

Rare earth double perovskites of the chemical formula  $R_2BB'O_6$  ( $R$  = rare earth,  $B/B'$  = transition metal) are actively investigated in recent times due to their potential to exhibit multiferroic and multifunctional properties. The research on double perovskites extends over bulk as well as thin films in order to realize usable multiferroic device elements [1, 2, 3, 4]. In addition to multiferroicity [2], observation of metamagnetic steps in magnetization [5], exchange bias [6], magnetoresistance and magnetocapacitance [7] make these compounds interesting. Several Mn and Ni – containing double perovskites [8] have been studied so far and their magnetic properties are understood in terms of the degree of cationic ordering and Goodenough-Kanamori (GK) rules [9] that predict ferromagnetism in these structures, or the deviations from GK rules due to inherent cationic disorder and subsequent departure from ferromagnetism. Usually, the double perovskite compounds prepared in the laboratory suffer from the inevitable antisite disorder due to cations interchanging their crystallographic positions. The formation of ordered structures demands suitable combination of  $R$  and/or  $B/B'$  cations with a proper control over synthesis parameters [10]. Fe-based double perovskites are less-investigated so far in spite of being an interesting class due to the possibility of exhibiting high temperature phase transitions. The double perovskites  $\text{Ho}_2\text{Fe}B'\text{O}_6$ , with a first row transition element at the  $B'$ -sites have distinct properties due to the  $3d$ - $3d$  and the  $3d$ - $4f$  interactions. In the case of  $B' = \text{Cr}$ , a crystallographically disordered antiferromagnet with tuned spin reorientation is found to occur [11] while for  $B' = \text{Mn}$ , a half metallic-ferrimagnet is predicted theoretically [12]. The Fe-Co combination has its own peculiarities due to their proximity in the periodic table with similar size and valence states. Realizing the potential of multifunctional properties and tunable physical properties in  $R_2BB'O_6$ , we carry out an experimental investigation of  $\text{Ho}_2\text{FeCoO}_6$  in the present paper.

The well-studied end members of  $\text{Ho}_2\text{FeCoO}_6$  are orthorhombic  $\text{HoFeO}_3$  and  $\text{HoCoO}_3$  [13, 14] which are weak ferromagnets with the rare earth  $\text{Ho}^{3+}$  ordering magnetically at  $\approx 4.1$  K and  $\approx 3$  K respectively [15, 13]. The orthoferrites  $R\text{FeO}_3$  generally have high Néel temperatures of the order of  $\sim 700$  K [16, 17] and in bulk form are not multiferroic though, recent theoretical calculations on thin films show the emergence of electric polarization with the application of strain [18]. In the orthoferrite  $\text{HoFeO}_3$  spin reorientation of the Fe moments is reported in the temperature ranges 50 K – 58 K [13] and 34 K – 54 K [19], caused by  $\text{Ho}^{3+} - \text{Fe}^{3+}$  interactions and competing Zeeman and van Vleck contribution to the anisotropy that initiates the Fe spin reorientation. When the  $B/B'$ -site is substituted with other transition metal cations like Cr or Mn, changes in the spin reorientation temperature are observed [20, 21]. In contrast to the orthoferrites, the orthocobaltites show lower values of Néel temperature which correspond to Ho ordering. Thus the combination of Co-Fe at the  $B/B'$ -site can tune the Néel temperatures to far below 700 K but well above 4 K. Unlike other orthocobaltites, where the  $\text{Co}^{3+}$  spins shows a transition from high spin (HS) to low spin (LS) via intermediate spin (IS)

states with decrease in temperature,  $\text{HoCoO}_3$  has its  $\text{Co}^{3+}$  in LS state [15], which is a diamagnetic state.

## 2. Experimental Methods

Phase-pure polycrystalline powders of  $\text{Ho}_2\text{FeCoO}_6$  were prepared through citrate route sol-gel method [22]. The phase purity of the synthesized powders were checked by doing Rietveld refinement [23] of the powder x ray diffractograms, recorded using a commercial x ray diffractometer (PANalytical X'Pert Pro), using the FullProf suite of programs [24]. About 4 g of  $\text{Ho}_2\text{FeCoO}_6$  was used for neutron powder diffraction experiments at BARC, Mumbai, India at the powder diffractometer (FCD-PD3), beam line TT-1015 of the Dhruva reactor using neutrons of wavelength, 1.48 Å [25]. Diffraction patterns were collected at 11 temperature points in the range 2.8 K to 300 K. The data was analysed using FullProf and the representation analysis of magnetic structures was carried out using BasIreps of FullProf suite [26],[27] and SARAH [28]. DC magnetic measurements were carried out using a commercial SQUID based VSM (MPMS 3, Quantum Design USA) in the temperature range 5 K to 375 K, in zero field-cooled warming (ZFC), field-cooled cooling (FCC) and field-cooled warming (FCW) protocols for various applied fields. Isothermal magnetization measurements for different temperatures were carried out up to 70 kOe. AC susceptibility measurements were performed with an ac amplitude of 2.5 Oe, at frequencies 0.3 Hz, 33 Hz, 333 Hz, 666 Hz and 999 Hz. Specific heat of  $\text{Ho}_2\text{FeCoO}_6$  was measured in zero field and in applied magnetic fields 10 kOe, 50 kOe and 80 kOe using a commercial Quantum Design PPMS instrument.

## 3. Results and discussion

### 3.1. Magnetization

The temperature dependence of DC magnetization of  $\text{Ho}_2\text{FeCoO}_6$  at an applied field of 100 Oe was performed following the protocol as ZFC  $\rightarrow$  FCC  $\rightarrow$  FCW. In the main panel of figure 1 (a) the field-cooled curves of the magnetization are presented as  $\Delta M = [M_{\text{FCW}} - M_{\text{ZFCW}}]$ , plotted as a function of temperature. The FCC and the FCW magnetization curves are presented in the inset of the figure. A phase transition from paramagnetic to antiferromagnetic phase occurs at  $T_{\text{N1}} \approx 250$  K. Also, a strong thermal hysteresis between the FCC and the FCW curves begins at  $T_{\text{N1}}$  as can be seen in the inset of figure 1(a). A second antiferromagnetic phase transition occurs at  $T_{\text{N2}} \approx 45$  K where a peak in magnetization and a subsequent sharp decrease occurs. Below  $T_{\text{N2}}$ , the magnetization tends to increase towards low temperature. This is attributed to the induced magnetism of  $\text{Ho}^{3+}$  polarized due to the ordering in the Fe/Co sub-lattice. A broad peak is seen at low temperature near 5 K suggesting short-range magnetic ordering of rare earth moments. The large region of thermal hysteresis (extended upto about 200 K) is probably due to the coexistence of symmetry-related structural phases or due to a multi-domain magnetic structure. It is interesting to note that orthoferrites

of general formula  $R\text{FeO}_3$  ( $R$  = rare earth), or their derivatives, are known to display spin reorientations and subsequently multi-domain magnetic structure that can show such hysteresis effects [29, 30]. In fact, a spin-reorientation transition occurs in the closely related compound  $\text{HoFeO}_3$  signified by twin peaks at 53 K and 58 K in specific heat [31, 32]. It is plausible that the phase transition seen in  $\text{Ho}_2\text{FeCoO}_6$  at  $T_{\text{N}2} \approx 45$  K is similar in nature.

From the presence of Ho in the compound, we assume time-independent susceptibility contributions due to diamagnetic and van Vleck terms to the total magnetic susceptibility of  $\text{Ho}_2\text{FeCoO}_6$ . Hence, a modified Curie-Weiss expression was used to analyse the magnetic susceptibility:

$$\chi_{\text{exp}} = \chi_o + \frac{C}{T - \theta_p} \quad (1)$$

Here,  $\chi_o$  represents the temperature-independent contributions,  $\theta_p$  is the Curie-Weiss temperature and  $C$  is the Curie constant. In figure 1 (b), the magnetic susceptibility of  $\text{Ho}_2\text{FeCoO}_6$  is given as  $\chi(T) = (\chi_{\text{exp}} - \chi_o)$  on the left axis and the corresponding inverse susceptibility on the right axis.  $\chi_o \sim 0.0286$  emu/mol-Oe was obtained from the fit on magnetic susceptibility using Eqn (1). A linear fit to  $1/(\chi_{\text{exp}} - \chi_o)$  vs  $T$  in the range of 275 K – 350 K was used to extract the effective paramagnetic moment and the Curie-Weiss temperature. Thus, an effective magnetic moment,  $\mu_{\text{eff}} = 11.74 \mu_{\text{B}}/\text{fu}$  with a Curie-Weiss temperature  $\theta_p = 90(3)$  K were obtained. The positive value of  $\theta_p$  suggest predominant ferromagnetic interactions. Interestingly, it can also be noted from the figure 1 (b) that extrapolating the linear fit to low temperatures would indicate the  $1/(\chi_{\text{exp}} - \chi_o)$  curve to behave similar to the Griffiths-like phase seen in double perovskites [33, 34, 35]. A mean-field approach to estimate the effective magnetic moment and Curie temperature need not essentially bring out the details of the complex magnetic interactions in  $\text{Ho}_2\text{FeCoO}_6$  as later on we see that prominent spin reorientation transitions exist in this material.

In the inset of figure 1 (b), we plot the derivative  $d\chi(T)/dT$  versus temperature to highlight the fact that the transition at  $T_{\text{N}2} \approx 45$  K is in fact a double transition. From  $d\chi(T)/dT$  we identify the two nearby transitions at  $T_1 \approx 44.5$  K and  $T_2 \approx 41.8$  K. This is reminiscent of the double-peak found in  $\text{HoFeO}_3$ [31]. Measurements on oriented single crystal samples might be essential to closely track the twin-peaks. With the application of external magnetic field, the phase transitions at  $T_{\text{N}1}$  and  $T_{\text{N}2}$  are observed to diminish. The ZFC magnetization is presented in figure 1 (c) where we can see that both the transitions vanish with the application of magnetic field of 70 kOe. An enlarged view of the region, 5 K – 80 K, around the transition is provided in the inset of the panel where the magnetic field is varied from 100 Oe to 70 kOe. These results support the predominant antiferromagnetic nature of the observed phase transitions in  $\text{Ho}_2\text{FeCoO}_6$ . In figure 2 (a), the real part of AC susceptibility  $\chi'(T)$  of  $\text{Ho}_2\text{FeCoO}_6$  measured with applied frequencies 0.3 Hz – 999 Hz in the temperature range 5 K – 100 K is presented. While the phase transition at  $T_{\text{N}2}$  is captured in  $\chi'(T)$ , no frequency dispersion is observed. The double peak that was observed in the  $d\chi/dT$  plots is not present in

$\chi'(T)$ . AC susceptibility of  $\text{Ho}_2\text{FeCoO}_6$  recorded with an applied frequency of 333 Hz and amplitude of 2.5 Oe, superposed with different DC fields (100 Oe – 70 kOe) is presented in the panel (b) of figure 2. In presence of a magnetic field, the peak at  $T_{\text{N}2}$  is found to be diminished. With the application of higher fields, 40 kOe and 70 kOe, it shifts to low temperatures and displays a broad peak. It could happen that the application of magnetic field suppressed one of the peaks at double transitions and enhanced the other. Or, in other words, one of the magnetic phases is being converted in to the other through a continuous rotation of spins [36, 37].

In figure 2 (c), the isothermal magnetization of  $\text{Ho}_2\text{FeCoO}_6$  is presented for temperatures in the range 5 K – 100 K. No sign of ferromagnetic saturation is seen attained at 5 K with the application of 70 kOe. Also, there is no indication of opening of a ferromagnetic loop. In Table 1, the possible combinations of the spins of Ho, Co and Fe in low spin (LS), intermediate spin (IS) and high spin (HS) states are given. The experimental saturation moment of  $\text{Ho}_2\text{FeCoO}_6$  at 5 K and 70 kOe was estimated from the law of approach to saturation as 11.2(4)  $\mu_{\text{B}}/\text{fu}$ . Comparing this experimental value with the effective moments resulting from the different combination in Table 1, it appears that  $\text{Ho}_2\text{FeCoO}_6$  has LS  $\text{Co}^{3+}$ , HS  $\text{Fe}^{3+}$  and paramagnetic  $\text{Ho}^{3+}$  spins.

### 3.2. Specific heat

The total specific heat  $C_p(T)$  of  $\text{Ho}_2\text{FeCoO}_6$  in 0 Oe, 10 kOe, 30 kOe, 50 kOe and 80 kOe are presented in the main panel of figure 3 (a). A broad peak centred at approximately 5 K arises from the magnetism of rare earth where the absence of a sharp  $\lambda$ -type anomaly suggests that the magnetic order in the Ho-sublattice might be of short-range type. We denote this anomaly as  $T_{\text{Ho}}$ . A peak is observed at  $T_{\text{N}1}$  (not shown) in the specific heat where the paramagnetic to antiferromagnetic phase transition happens. At  $T_{\text{N}2} \approx 45$  K, the  $C_p(T)$  displays a peak which arises from the spin reorientation of the Fe moments. The inset of figure 3(a) provides a plot of  $dC_p/dT$  versus temperature, highlighting the magnetic phase transitions at  $T_{\text{N}1}$  and  $T_{\text{N}2}$ . The zero field specific heat in the inset confirms that the anomaly at  $T_{\text{N}2}$  indeed has a double-peak structure as was observed in the DC magnetic susceptibility. Also evident from the inset is the fact that the peak in  $C_p(T)$  at 45 K is diminished with the application of external magnetic field – an indication that antiferromagnetic interactions are important in this compound. On the other hand, the specific heat at  $T_{\text{Ho}}$  is enhanced with the application of magnetic field, especially, 50 kOe and 80 kOe. The low temperature region (from 15 K – 30 K) of the specific heat of  $\text{Ho}_2\text{FeCoO}_6$  is fitted using the expression  $C_p(T) = \beta T^3 + \alpha T^5 + \gamma T$ , where the terms containing  $\alpha$  and  $\beta$  correspond to phonon contribution while the term with  $\gamma$  describes the electronic part. The specific heat data in zero and applied fields are fitted to this expression and the resulting fit parameters are shown in Table 2. The fit so obtained for the 10 kOe specific heat data is shown in figure 3 (c) as a solid line. Using the value of  $\beta$ , the Debye temperature is then estimated as  $\theta_{\text{D}} = \left( \frac{12p\pi^4 R}{5\beta} \right)^{1/3}$  where  $p$  is the number of atoms in unit cell and  $R$  is the universal gas constant. In the

low temperature region,  $\theta_D = 138$  K is obtained for  $\text{Ho}_2\text{FeCoO}_6$ .

The specific heat of  $\text{Eu}_2\text{FeCoO}_6$  is plotted in the main panel of figure 3 (a) as a black solid line. Using this as the non-magnetic analogue ( $\text{Eu}^{3+}$  being diamagnetic) and subtracting it from the specific heat of  $\text{Ho}_2\text{FeCoO}_6$  we recover the magnetic specific heat corresponding to  $\text{Ho}^{3+}$ . This quantity,  $\Delta C_p = (C_p(\text{Ho}_2\text{FeCoO}_6) - C_p(\text{Eu}_2\text{FeCoO}_6))$  for the temperature range 2 K to 100 K is plotted in figure 3 (b). In addition to the broad peak at  $T_{\text{Ho}}$  due to the short-range magnetic order in the Ho sub-lattice,  $\Delta C_p$  also recovers a Schottky-like peak for  $\text{Ho}_2\text{FeCoO}_6$  centred at around 50 K ( $T_{\text{Sch}}$ ) which is similar to the case of  $\text{HoFeO}_3$ [31]. The spin reorientation of the Fe spins appears as a sharp peak at 45 K. We analyze the Schottky-like peak of  $\Delta C_p$  by using a multi-level crystal field model similar to that used in the case of  $\text{HoFeO}_3$ [31]. The fit obtained in the case of  $\text{Ho}_2\text{FeCoO}_6$  is shown as a solid line in figure 3 (b). An 8 level crystal field model was found to roughly account for the Schottky-like peak centred at  $T_{\text{Sch}}$ . The temperature ranges 15 K – 40 K and 50 K – 60 K were used for the fit, thereby avoiding the region near the peak at  $T_{\text{N}2}$ . From the fit we estimate crystal field energy levels as 0 K, 79 K, 160 K (doublet), 165 K, 672 K (doublet) and 683 K. Though a detailed estimation of the crystal field levels would require neutron inelastic scattering experiments, the values that we provide here are from a first-principles curve fit assuming the values for that of  $\text{HoFeO}_3$  as a starting point. In the case of  $\text{HoFeO}_3$  the low symmetry of the Ho position leads to the assumption of 17 independent crystal field levels. Bhattacharjee *et al.*, [38] reports 0 K (doublet), 110 K (degeneracy = 2), 230 K (4), 330 K (2) and 700 K (7) through a trial-and-error curve fit.

The magnetic entropy of  $\text{Ho}_2\text{FeCoO}_6$  is estimated from  $\Delta C_p$  as  $S_{\text{mag}} = \int (\Delta C_p/T) dT$  and is plotted in figure 3 (c). Two horizontal black lines in the graph indicate the location of  $R \ln(2)$  and  $R \ln(17)$ . It can be seen that the transition at  $T_{\text{Ho}}$  recovers entropy close to  $R \ln(2)$  suggesting a doublet, which was the case in  $\text{HoFeO}_3$ [31]. Thus, combining ac and dc magnetization and specific heat, we identify two magnetic phase transitions in  $\text{Ho}_2\text{FeCoO}_6$  at 250 K and at 45 K and also signature of short-range magnetic order of the rare earth at 5 K. The transition at 45 K is identified as a spin reorientation transition. In order to confirm this and to obtain the details of the crystal and magnetic structure, we proceed now to analyze the neutron diffraction data obtained on  $\text{Ho}_2\text{FeCoO}_6$ .

### 3.3. Neutron diffraction

The neutron diffraction pattern of  $\text{Ho}_2\text{FeCoO}_6$  obtained at 300 K is shown in figure 4 (a). Our first attempt was to understand the crystal structure, especially the degree of ordering of Fe and Co. Generally, the double perovskites crystallize in ordered arrangement for Fe and Co and subsequently the crystal structure is described in the monoclinic space group  $P2_1/n$  where Fe and Co occupy the  $2c$  and  $2d$  Wyckoff positions, respectively. If the cations are disordered, they occupy a common  $4b$  position and can be described using the space group  $Pbnm$ . The difference in coherent neutron scattering lengths of Fe (9.45 fm) and Co (2.49 fm) would allow the estimation of the degree of

cation ordering, if studied using neutron scattering. Hence, our first attempt was to refine the diffraction data in the cation-ordered  $P2_1/n$  space group. However, if the cations are ordered in the double perovskite structure, it leads to the appearance of (011) peak in the diffracted intensity [39]. The absence of such a peak in the neutron diffraction data of  $\text{Ho}_2\text{FeCoO}_6$  suggested that the degree of ordering is very low in this compound. Hence, we used  $Pbnm$  as the structural model for  $\text{Ho}_2\text{FeCoO}_6$  where Fe and Co are randomly occupied on 6c crystallographic position. The Rietveld fit to the 300 K-data is presented in figure 4 (a) as a solid line. The refined atomic positions at 300 K obtained via the refinement are given in Table 3. The temperature dependence of lattice parameters and the unit cell volume (refer Table 4) is presented in panels (c),(d),(e) and (f) of figure 4. Thermal expansion of the unit cell volume is observed with temperature. The anomaly present in the magnetic data referring to the spin reorientation transition is also reflected in the thermal evolution of unit cell volume. This indicates a close connection between the spin reorientation and the lattice effects in this material.

From the magnetisation data presented in Section 3.1, we know that a magnetic phase transition from paramagnetic to an antiferromagnetic phase occurs at  $T_{N1} \approx 250$  K. Hence, below  $T_{N1}$ , the neutron diffraction data is refined by adding a magnetic phase also to the nuclear structure. The emergence of the magnetic long-range order is evident in the neutron diffraction data from the development of diffracted intensity of the (110) peak that builds up from 200 K down towards 44 K, see figure 4 (b). Below 44 K, the intensity of the (101) peak diminishes while that of (110) is enhanced. This gives the first indication that  $\text{Ho}_2\text{FeCoO}_6$  undergoes a change in magnetic structure as a function of temperature. In order to analyse the magnetic structure of  $\text{Ho}_2\text{FeCoO}_6$  from the diffraction pattern at 200 K, we determined the propagation vector from profile fits to the magnetic peak at (011) and subsequently using the  $k$ -search utility in FullProf. The irreducible representations (IR) of symmetry allowed magnetic structures for  $Pbnm$  space group were obtained using the softwares, BasIreps of FullProf suite [26],[27] and SARA $h$  [28]. Four IR's were suggested -  $\Gamma_1$ ,  $\Gamma_3$ ,  $\Gamma_5$  and  $\Gamma_7$ . Each of the four magnetic representations was tried in a trial-and-error method to do a Rietveld fit for the 200 K data. We found that the representations  $\Gamma_1$  and  $\Gamma_3$  described the data well. However the best fit to the data was obtained for the mixed magnetic phase ( $\Gamma_1 + \Gamma_3$ ). This result also supports the preliminary deduction from the thermal hysteresis seen in the dc magnetization that the compound  $\text{Ho}_2\text{FeCoO}_6$  consists of mixed magnetic structures in the temperature range from 200 K to at least 45 K ( $T_{N2}$ ). In fact, the refinement of the diffraction data at low temperatures show that the mixed magnetic phase exists in the entire temperature region of 200 K to  $T_{N2} \approx 45$  K where the spin reorientation transition occurs. Below  $T_{N2}$ , only one magnetic phase exists -  $\Gamma_1$ . Thus the spin reorientation transition in  $\text{Ho}_2\text{FeCoO}_6$  is characterized by the transformation from ( $\Gamma_1 + \Gamma_3$ ) to  $\Gamma_1$ . It is seen in the inset of figure 1 (a) that the thermal hysteresis also terminates at  $T_{N2}$ . At 2.8 K, we analysed the diffraction data to include the magnetic long-range order in the Ho sub-lattice also. However, adding a magnetic phase to Ho in the refinement did not

improve the fit or did not better the  $\chi^2$  of fit. Moreover, from the magnetization and the specific heat data no sign of long range order was suggested for Ho. The Rietveld refined neutron diffraction data at 200 K, 45 K and 2.8 K are shown in figure 5 (a), (b) and (c) respectively and the magnetic structure formed by the Fe/Co moments are shown in (d) and (e). The magnetic moment values obtained at temperatures below 44 K are presented in right most column of table 4. The existence of mixed magnetic phases in the sample from 44 K made it difficult to estimate the accurate moment values for the experimented temperatures at and above 44 K. In addition, the neutron diffraction data below 10 K show significant enhancement of the intensity in the low-angle region as a broad peak. The diffracted intensity is plotted in figure 5 (f) to show the difference patterns (102 K – 300 K), (35 K – 300 K) and (2.8 K – 300 K). It can be seen that at 2.8 K, broad diffuse scattering emerges in the difference pattern. This is a clear indication of the short-range diffuse magnetic scattering from  $\text{Ho}^{3+}$ . Hence, we affirm that the  $\text{Ho}^{3+}$  moment does not order completely long range in  $\text{Ho}_2\text{FeCoO}_6$  down to 2.8 K.

#### 4. Conclusions

The double perovskite compound  $\text{Ho}_2\text{FeCoO}_6$  displays two magnetic phase transitions, one at  $T_{\text{N1}} \approx 250$  K and the second at  $T_{\text{N2}} \approx 45$  K. The first transition marks the paramagnetic to antiferromagnetic mixed-phase region where the magnetic structure is described by the representation  $(\Gamma_1 + \Gamma_3)$  which is antiferromagnetic. After coexisting for a large temperature range, the mixed magnetic structure undergoes a spin reorientation and transforms to pure  $\Gamma_1$  phase at  $T_{\text{N2}}$ . Though the signature of long-range magnetic order is clear in the transition metal lattice, only short-range magnetic order exists in the  $\text{Ho}^{3+}$ -lattice.

#### Acknowledgements

HGR acknowledges Prof. A. M. Strydom and Dr. K. Ramesh Kumar (Highly Correlated Matter Research Group, University of Johannesburg, South Africa) for zero field HC measurement on  $\text{Eu}_2\text{FeCoO}_6$ , Dr. Radhika V. Nair (IIT Madras) for constant help and support provided during sample synthesis and Mr. P. Seenivasan (IIT Madras) for the help during SVSM experiments.

## References

- [1] Singh M P, Truong K D, Jandl S and Fournier P 2010 *J. Appl. Phys.* **107** 09D917
- [2] Yáñez Vilar S, Mun E D, Zapf V S, Ueland B G, Gardner J S, Thompson J D, Singleton J, Sánchez-Andújar M, Mira J and Biskup N 2011 *Phys. Rev. B* **84** 134427
- [3] Ramesh R and Spaldin N A 2007 *Nature Mater.* **6** 21–29
- [4] Kobayashi K I, Kimura T, Sawada H, Terakura K and Tokura Y 1998 *Nature* **395** 677–680
- [5] Nair H S, Pradheesh R, Xiao Y, Cherian D, Elizabeth S, Hansen T, Chatterji T and Brückel T 2014 *J. Appl. Phys.* **116** 123907
- [6] Nair H S, Chatterji T and Strydom A M 2015 *Appl. Phys. Lett.* **106** 022407
- [7] Rogado N S, Li J, Sleight A W and Subramanian M A 2005 *Adv. Mater.* **17** 2225–2227
- [8] Booth R J, Fillman R, Whitaker H, Nag A, Tiwari R M, Ramanujachary K V, Gopalakrishnan J and Lofland S E 2009 *Mater. Res. Bull.* **44** 1559–1564
- [9] Goodenough J B 1955 *Phys. Rev.* **100** 564
- [10] Sarma D D, Sampathkumaran E V, Ray S, Nagarajan R, Majumdar S, Kumar A, Nalini G and Row T N G 2000 *Solid State Communications* **114** 465–468
- [11] Kotnana G and Jammalamadaka S N 2015 *J. Appl. Phys.* **118** 124101
- [12] Zhang J T, Lu X M, Zhou J, Su J, Min K L, Huang F Z and Zhu J S 2010 *Phys. Rev. B* **82** 224413
- [13] Shao M, Cao S, Wang Y, Yuan S, Kang B, Zhang J, Wu A and Xu J 2011 *J. Cryst. Growth* **318** 947–950
- [14] Alonso J A, Martínez-Lope M J, de La Calle C and Pomjakushin V 2006 *J. Mater. Chem.* **16** 1555–1560
- [15] Muñoz A, Martínez-Lope M J, Alonso J A and Fernández-Díaz M T 2012 *European Journal of Inorganic Chemistry* **2012** 5825–5830
- [16] Marezio M, Remeika J P and Dernier P D 1970 *Acta Crystallogr. B* **26** 2008–2022
- [17] Eibschütz M, Shtrikman S and Treves D 1967 *Phys. Rev.* **156** 562
- [18] Zhao H J, Ren W, Yang Y, Chen X M and Bellaiche L 2013 *J. Phys.: Condens. Matter* **25** 466002
- [19] Nikolov O, Ruskov T, Vorobyov G P, Kadomtseva A M and Krynetskii I B 1990 *Hyper. Inter.* **54** 623–626
- [20] Yuan S, Yang Y, Cao Y, Wu A, Lu B, Cao S and Zhang J 2014 *Solid State Commun.* **188** 19–22
- [21] Kotnana G and Jammalamadaka S N 2016 *J. Mag. Mag. Mater.* **418** 81–85
- [22] Haripriya G R, Pradheesh R, Singh M N, Sinha A K, Sethupathi K and Sankaranarayanan V 2017 *AIP Advances* **7** 055826
- [23] Rietveld H M 1969 *J. Appl. Crystallogr.* **2** 65–71
- [24] Rodriguez-Carvajal J *Laboratoire Léon Brillouin, Saclay, France* URL <https://www.ill.eu/sites/fullprof/>
- [25] Siruguri V, Babu P D, Gupta M, Pimpale A V and Goyal P S 2008 *Pramana J. Phys* **71** 1197
- [26] Rodriguez-Carvajal J 2011 *Solid State Phenom.* **170** 263
- [27] Ritter C 2011 Neutrons not entitled to retire at the age of 60: More than ever needed to reveal magnetic structures *Solid State Phenom.* vol 170 (Trans Tech Publ) pp 263–269
- [28] Wills A S 2000 *Physica B* **276** 680–681
- [29] White R L 1969 *J. Appl. Phys.* **40** 1061–1069
- [30] Nair H S, Chatterji T, Kumar C M N, Hansen T, Nhalil H, Elizabeth S and Strydom A M 2016 *J. Appl. Phys.* **119** 053901
- [31] Bhattacharjee A, Saito K and Sorai M 2002 *J. Phys. Chem. Solids* **63** 569–574
- [32] Saito K, Sato A, Bhattacharjee A and Sorai M 2001 *Solid State Commun.* **120** 129–132
- [33] Nair H S, Swain D, Adiga S, Narayana C and Elizabeth S 2011 *J. Appl. Phys.* **110** 123919
- [34] Liu W, Shi L, Zhou S, Zhao J, Li Y and Guo Y 2014 *J. Appl. Phys.* **116** 193901
- [35] Chakraborty T, Nair H S, Nhalil H, Kumar K R, Strydom A M and Elizabeth S 2016 *J. Phys.: Condens. Matter* **29** 025804
- [36] Belov K P, Zvezdin A K, Kadomtseva A M and Levitin R 1976 *Sov. Phys. Usp.* **19** 574

- [37] Gorodetsky G and Levinson L M 1969 *Solid State Commun.* **7** 67–70
- [38] Banerjee B K 1964 *Physics letters* **12** 16–17
- [39] Barón-González A J, Frontera C, García-Muñoz J L, Rivas-Murias B and Blasco J 2011 *J. Phys.: Condens. Matter* **23** 496003
- [40] Momma K and Izumi F 2011 *Journal of Applied Crystallography* **44** 1272–1276

**Table 1.** The effective magnetic moment values of  $\text{Ho}_2\text{FeCoO}_6$  (calculated theoretically considering the paramagnetic moments of the constituent cations viz., spin only moments of Fe, and Co and spin-orbit coupling of Ho), assuming different valence states (V) and spin states (SS) for Ho, Co and Fe. The magnetic moment values are given in the units of  $\mu_B$ . The total moment  $\mu_{\text{tot}}$  is estimated as  $\sqrt{\mu_{\text{Ho}}^2 + 0.5(\mu_{\text{Fe}}^2 + \mu_{\text{Co}}^2)}$ . (LS: low spin, IS: intermediate spin and HS: high spin).

$\text{Ho}^{3+}$ ( $\mu_{\text{Ho}}$ )	Co (V, SS, $\mu_{\text{Co}}$ )	Fe (V, SS, $\mu_{\text{Fe}}$ )	$\mu_{\text{tot.}}$ ( $\mu_B$ )
10.6	+3, LS, 0	+3, LS, 1.73	10.67
		+3, HS, 5.92	11.39
		+4, LS, 2.82	10.79
		+4, HS, 4.89	11.15
10.6	+3, IS, 2.82	+3, LS, 1.73	10.86
		+3, HS, 5.92	11.56
		+4, LS, 2.82	12.01
		+4, HS, 4.89	11.32
10.6	+3, HS, 4.89	+3, LS, 1.73	11.22
		+3, HS, 5.92	11.91
		+4, LS, 2.82	11.33
		+4, HS, 4.89	11.67
10.6	+4, LS, 1.73	+3, LS, 1.73	10.74
		+3, HS, 5.92	11.46
		+4, LS, 2.82	11.33
		+4, HS, 4.89	11.22
10.6	+4, HS, 5.92	+3, LS, 1.73	11.46
		+3, HS, 5.92	12.14
		+4, LS, 2.82	11.57
		+4, HS, 4.89	11.91

**Table 2.** The fit parameters obtained by analysing the low temperature specific heat of  $\text{Ho}_2\text{FeCoO}_6$  in the temperature range 15 K – 30 K. The Sommerfeld coefficient  $\gamma$  and the Debye temperature  $\theta_D$  estimated from the fit are shown.

H (T)	$\alpha$ ( $10^{-8}$ J/mol K $^{-6}$ )	$\beta$ ( $10^{-4}$ J/mol K $^{-4}$ )	$\gamma$ (J/mol K $^{-2}$ )	$\theta_D$ (K)
0	-19.0	72.9	0.128	138
1	-14.8	6.57	0.160	-
5	-8.89	4.74	0.343	-
8	-23.6	7.36	0.271	-

**Table 3.** The fractional coordinates of atoms in  $\text{Ho}_2\text{FeCoO}_6$  at 300 K according to  $Pbnm$  space group setting.

	$x$	$y$	$z$	$B_{\text{iso}}$
Ho	0.9862(9)	0.0689(5)	0.25	0.0073
Co/Fe	0.5	0	0	0.0085
Fe/Co	0.5	0	0	0.0085
O(1)	0.0995(9)	0.4724(9)	0.25	0.0136
O(2)	0.6943(8)	0.2994(8)	0.0526(5)	0.0147

**Table 4.** The lattice parameters and the magnetic moments extracted using Rietveld refinement of neutron diffraction data.

$T$ (K)	$a$ (Å)	$b$ (Å)	$c$ (Å)	$V$ (Å <sup>3</sup> )	Magnetic moment( $\Gamma_1$ ) $\mu_B$
2.8	5.2071(2)	5.5020(3)	7.4696(4)	214.000(19)	3.2(1)
10	5.2070(2)	5.5015(3)	7.4703(3)	213.997(18)	3.5(1)
35	5.2069(2)	5.5013(3)	7.4702(3)	213.981(16)	3.0(1)
38	5.2071(2)	5.5014(3)	7.4700(3)	213.988(16)	3.4(1)
40	5.2070(2)	5.5017(3)	7.4703(3)	214.004(18)	3.2(1)
42	5.2072(2)	5.5017(3)	7.4701(3)	214.007(18)	3.7(1)
44	5.2072(2)	5.5012(3)	7.4704(3)	213.995(16)	2.7(2)
50	5.2072(2)	5.5016(3)	7.4704(3)	214.011(17)	
102	5.2080(2)	5.5017(3)	7.4721(3)	214.097(18)	
200	5.2110(2)	5.5028(3)	7.4775(3)	214.419(18)	
300	5.2159(1)	5.5048(9)	7.4846(6)	214.897(21)	

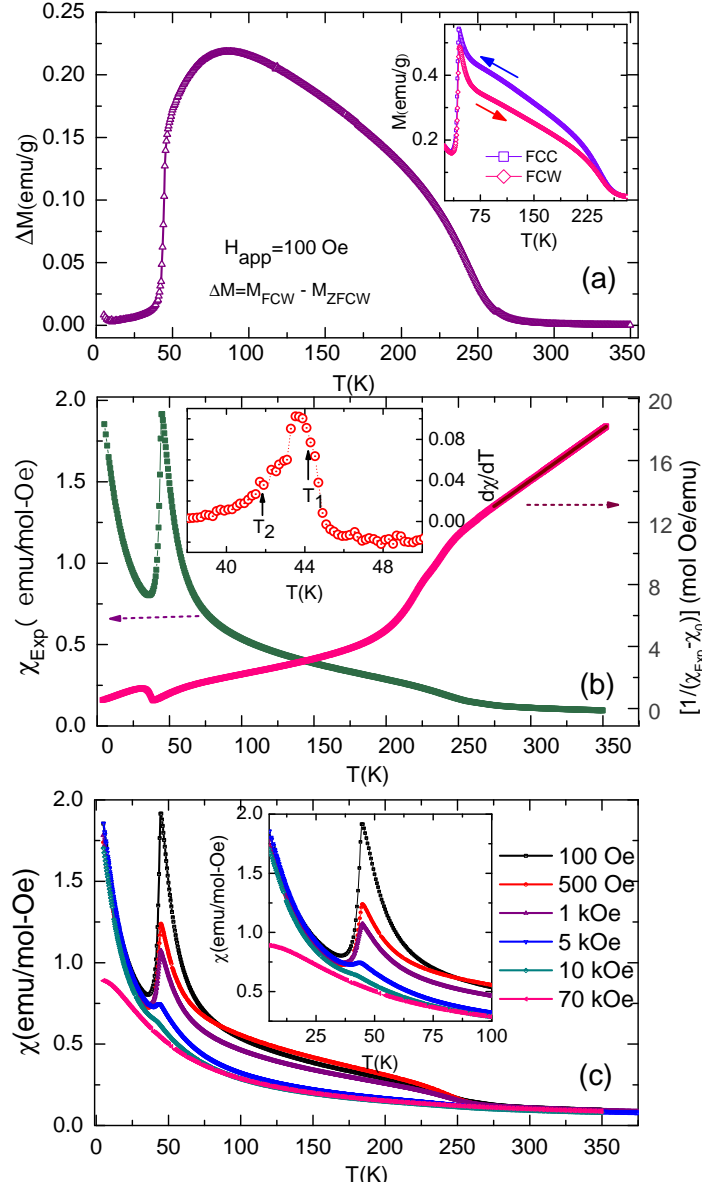


**Figure 1.** (colour online) (a) The temperature-dependent magnetization of  $\text{Ho}_2\text{FeCoO}_6$  at an applied field of 100 Oe plotted as  $M_{\text{FCW}} - M_{\text{ZFCW}}$ . Magnetic phase transitions occur at  $T_{N1} \approx 250$  K and  $T_{N2} \approx 45$  K. The FCC and FCW arms of magnetization are presented in the inset. A large thermal hysteresis over a wide temperature range of 250 K - 50 K. (b) The susceptibility  $\chi(T) = [\chi_{\text{exp}} - \chi_0]$  and the corresponding inverse susceptibility at 100 Oe magnetic field. The black solid line is the fit according to ideal Curie-Weiss law. The inset shows  $d\chi/dT$  where a twin-peak is identified at  $T_{N2}$ . (c) The effect of applied field on the magnetic phase transitions are indicated.

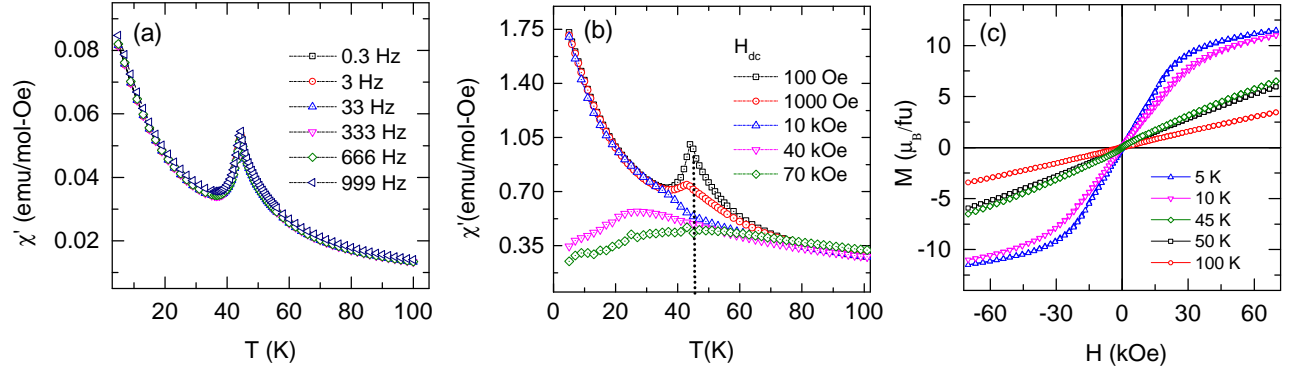


**Figure 2.** (colour online) (a) No frequency dependence of the real part of ac susceptibility,  $\chi'(T)$  over 0.3 Hz to 999 Hz is observed at  $T_{N2}$  for  $\text{Ho}_2\text{FeCoO}_6$ . (b) With a superposed DC magnetic field, the peak at  $T_{N2}$  is observed to get suppressed while slightly shifting to the low temperatures. The vertical dash-dotted line is drawn to indicate this shift. (c) The isothermal magnetization at different temperatures in the range 5 K to 100 K.

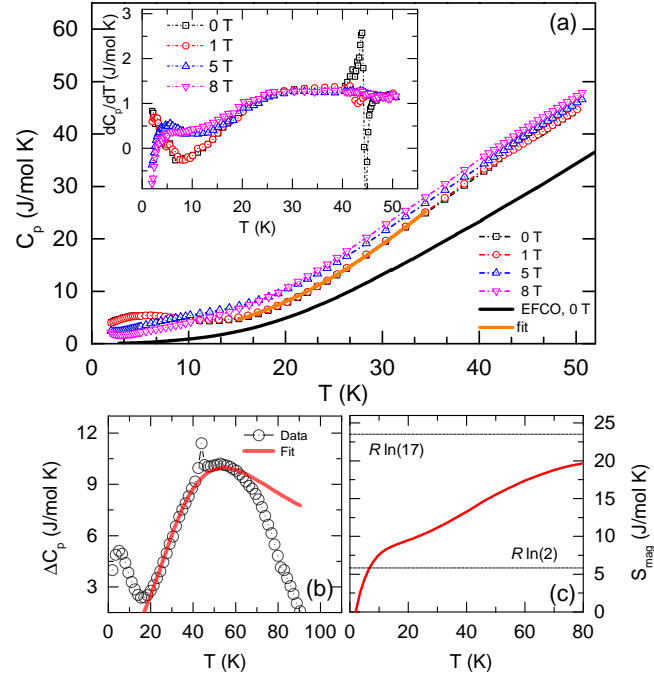


**Figure 3.** (color online) (a) The specific heat of  $\text{Ho}_2\text{FeCoO}_6$  in zero and applied fields of  $H = 10$  kOe, 50 kOe and 80 kOe in the temperature range 2 K - 50 K. The phase transition at  $T_N$  is clearly seen at  $\approx 45$  K and the rare earth magnetism as a broad peak at  $\approx 5$  K. With the application of the field, the peak at 45 K is suppressed. The low temperature fit (15 K - 35 K) is shown as an orange solid line. The inset is a plot of  $dC_p/dT$  versus  $T$ . (b) The  $\Delta C_p$  is plotted along with a fit using a Schottky model of 7 crystal field levels. (c) The magnetic entropy  $S_{\text{mag}}$  estimated from  $\Delta C_p$ .

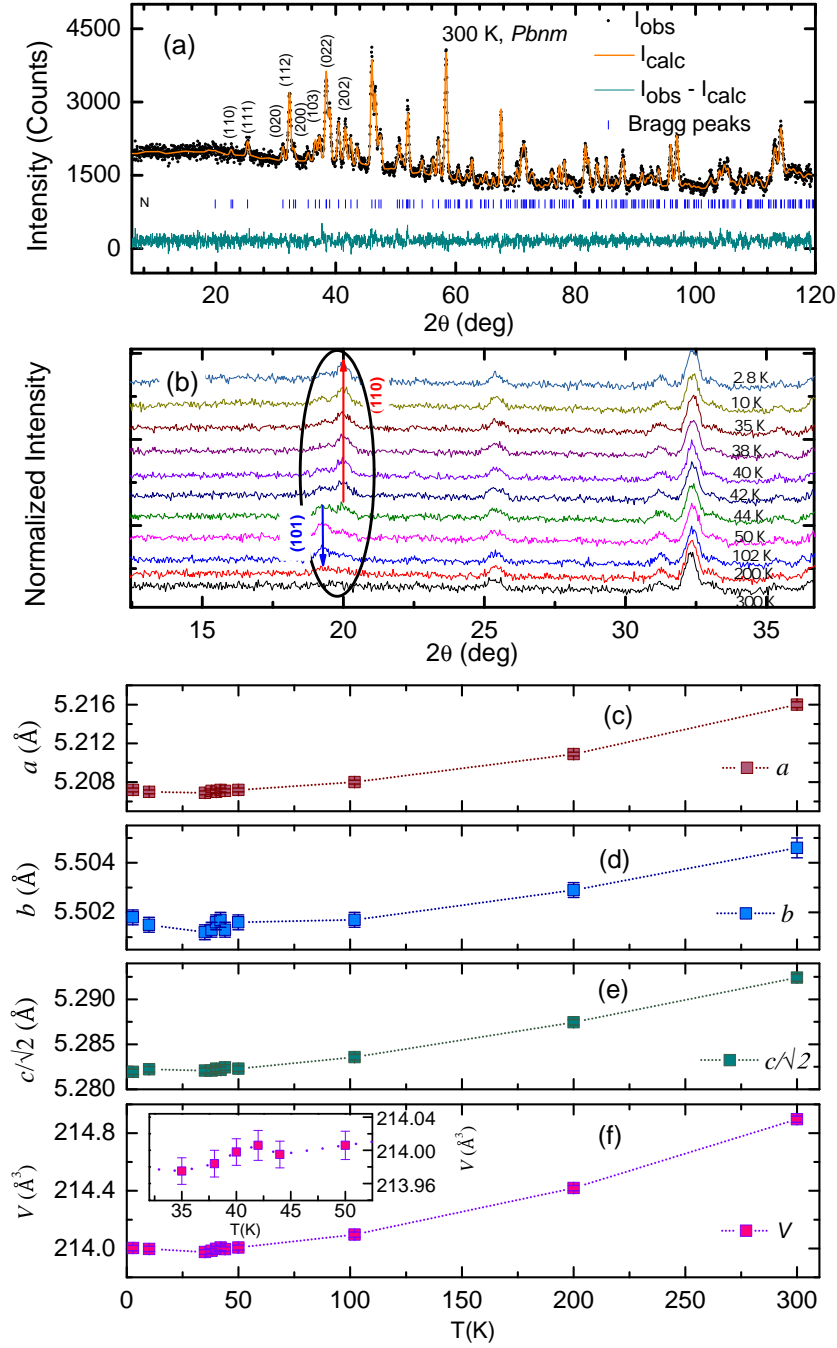


**Figure 4.** (color online) (a) The neutron diffraction data of  $\text{Ho}_2\text{FeCoO}_6$  at 300 K. The experimental data are shown in dark circles and the Rietveld fits assuming  $Pbnm$  space group are shown as orange lines. (b) The temperature evolution of the neutron diffraction patterns from 300 K to 2.8 K. The intensity of the (101) peak increases from 44 K to 200 K; below 44 K the intensity shifts to the (110) peak. (c)-(e) The temperature dependence of lattice parameters  $a$ ,  $b$  and  $c$  respectively. (f) The main panel shows temperature evolution of unit cell volume  $V$ , inset shows the anomaly observed around  $T_{N2}$ .

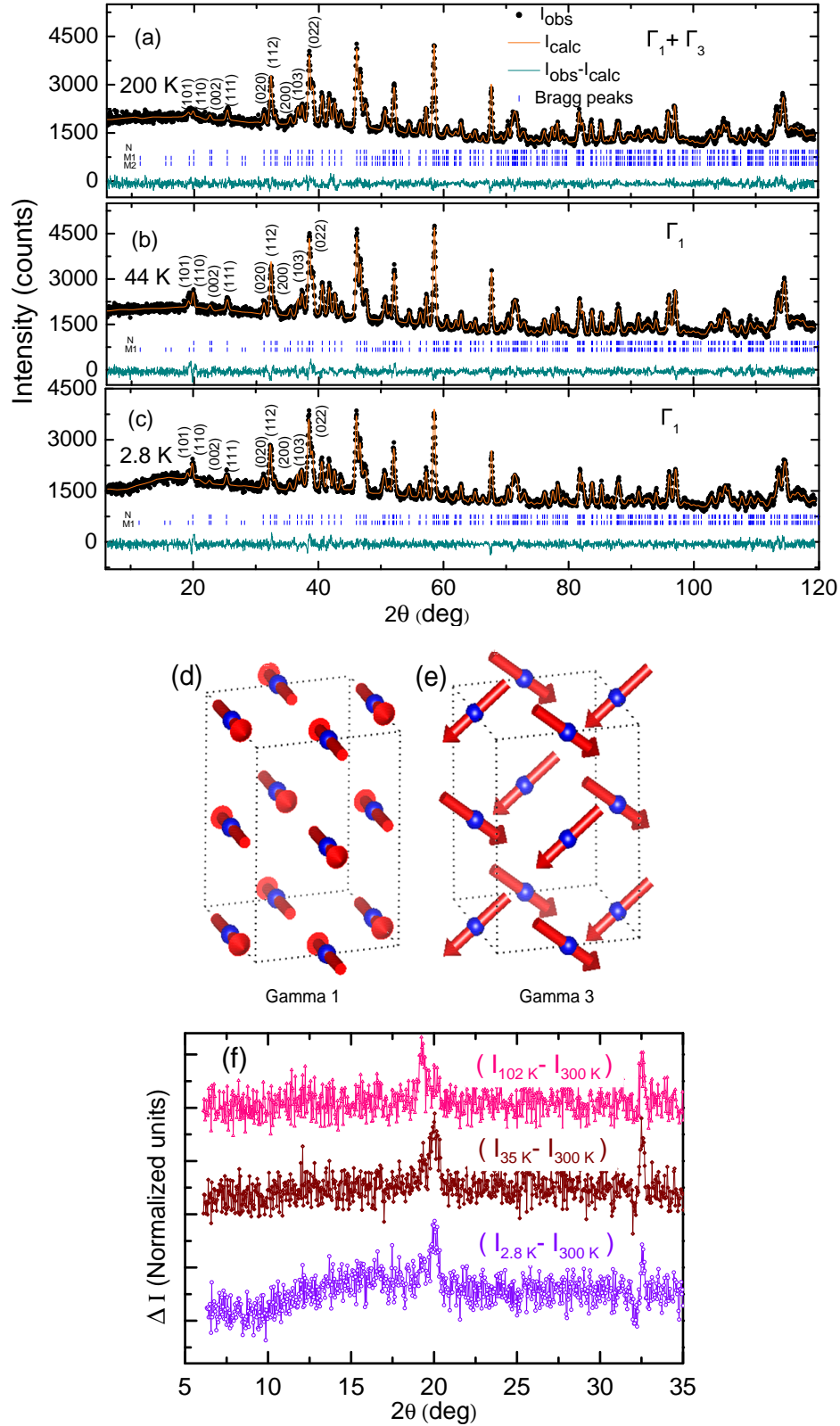


**Figure 5.** (colour online) (a) The neutron diffraction intensity of  $\text{Ho}_2\text{FeCoO}_6$  at (a) 200 K (b) 44 K and (c) 2.8 K presented along with the results of Rietveld refinement. At 200 K the magnetic structure consists of the mixed phase ( $\Gamma_1 + \Gamma_3$ ). At 44 K, the mixed phase transforms to a single phase  $\Gamma_1$  and this phase remains down till 2.8 K. The magnetic structures of (d)  $\Gamma_1$  and (e)  $\Gamma_3$ , visualized using VESTA [40]. (f) The diffuse scattering signal obtained at 102 K, 35 K and 2.8 K by subtracting the 300 K data.